

https://doi.org/10.1070/QEL17251

Detection of coherent optical phonons in a thin bismuth film by ultrafast electron diffraction

B.N. Mironov, S.A. Aseyev, A.A. Ischenko, I.V. Kochikov, S.V. Chekalin, E.A. Ryabov

Abstract. **Coherent dynamics of lattice oscillations in a ~20-nm-thick film obtained by thermal sputtering of bismuth is studied using ultrashort electron bunches synchronised with femtosecond laser pulses irradiating the sample. The Fourier analysis of ultrafast electron diffraction (UED) data shows that the observed modulation of the signal is due to the ensemble of modes corresponding to optical phonons with frequencies of approximately 3, 6 and 9 THz. A conclusion is made that these peaks correspond to the manifestation of the bismuth A_{1g} mode (three-terahertz peak), as well as its first and second overtones, which is probably due to quantum confinement in a 20-nm Bi nanostructure. The possibility of a detailed study of the quantum-size effect in bismuth with the help of a transmission UED is analysed.**

Keywords: *ultrafast electron diffraction, femtosecond laser radiation, optical phonons, thin bismuth film.*

1. Introduction

Ultrafast electron diffraction (UED) is a powerful tool for studying fast processes and structural phase laser-stimulated transitions in physics, chemistry and biology on their natural spatiotemporal scales [1–6]. In contrast to purely optical pump–probe methods, the use of ultrashort electron probe pulses allows one to obtain direct information about the structural dynamics directly from the time-dependent diffraction pattern. Earlier, we used UED to detect coherent optical phonons in a thin antimony film [7, 8], where the efficiency of their generation under the action of femtosecond laser radiation is quite high. Note that Sb crystallises in the rhombohedral structure of A7 with two atoms in the unit cell, a 'bismuth-type lattice'. The crystal structure of bismuth is described in detail in Ref. [9].

Bismuth, like antimony, is a model object for real-time studies of the various stages of the oscillatory motion of a lattice of a solid body induced by ultrashort laser pulses [10]. In the framework of this direction, a series of works has been arried out to examine the relaxation dynamics of a crystalline bismuth lattice due to oscillations of the A_{1g} optical phonon mode by of laser pump–probe method [11–17] (see also references in [17]). The use of UED made it possible to visualise nonthermal melting [18], as well as coherent low-frequency acoustic phonons in a thin bismuth film [19], which demonstrated the feasibility of this method to directly measure the ultrafast relaxation dynamics of the crystalline Bi structure at its natural time scales. When working with films, it is important to take into account the fact that quantum confinement and accompanying changes in the electronic structure (from a semiconductor in thin films ~30–40 nm thick and less to a semimetal in bulk samples [20, 21]) for this material can have a noticeable effect on the laser-induced response [16].

In the present work, the nonequilibrium excited state of the lattice in a thin bismuth film was produced by high-power femtosecond laser radiation. Pulse heating of the lattice due to electron–phonon interaction was accompanied by the formation of high-frequency optical phonons. In the experiment, these oscillations were recorded by the UED method.

2. Experiment

Figure 1 shows the schematic of a femtosecond electron diffractometer [6–8]. To probe ultrafast processes in a solid-state sample, we used photoelectron pulses generated by irradiation of a cathode with femtosecond laser light. The cathode was made of a semitransparent (~30 nm thick) gold layer on a quartz plate irradiated by the third harmonic of a Ti : sapphire laser with a wavelength λ = 266 nm, while the fundamental harmonic with λ = 800 nm and a pulse duration of 50 fs was used to pump the sample. Optical and photoelectron pulses were precisely synchronised using the same femtosecond Ti:sapphire laser for pump and probe channels.

An electron beam with an energy of 20 keV and a diameter of 100 μm was formed by a permanent magnet lens. The employed scheme made it possible to minimise the spreading of electron bunches due to a small (12 mm) distance from the photocathode to the sample, which is important for enabling the high temporal resolution of UED. An assembly based on a microchannel plate (MCP) and a phosphor screen was used to register electrons and to obtain a two-dimensional image of the signal. Then, the data was read by a CCD camera and transferred to a computer for processing.

As a sample we used a ~20-nm-thick bismuth film deposited by thermal sputtering on a carbon substrate used in transmission electron microscopy, and then placed to the electron diffractometer chamber. The presence of distinct rings in the diffraction pattern recorded with a pulsed photoelectron beam in the absence of optical pumping is due to the

B.N. Mironov, S.A. Aseyev, S.V. Chekalin, E.A. Ryabov Institute for Spectroscopy, Russian Academy of Sciences, ul. Fizicheskaya 5, 108840 Moscow, Troitsk, Russia; e-mail: isanfemto@yandex.ru, ryabov@isan.troitsk.ru;
A.A. Ischenko Russian Technological University (MIREA), Lomonosov Institute of Fine Chemical Technologies, prosp. Vernadskogo 86, 119571 Moscow, Russia;
I.V. Kochikov Faculty of Physics, Lomonosov Moscow State University, Vorob'evy gory, 119234 Moscow, Russia

Received 29 January 2020
Kvantovaya Elektronika **50** (3) 242–245 (2020)
Translated by I.A. Ulitkin

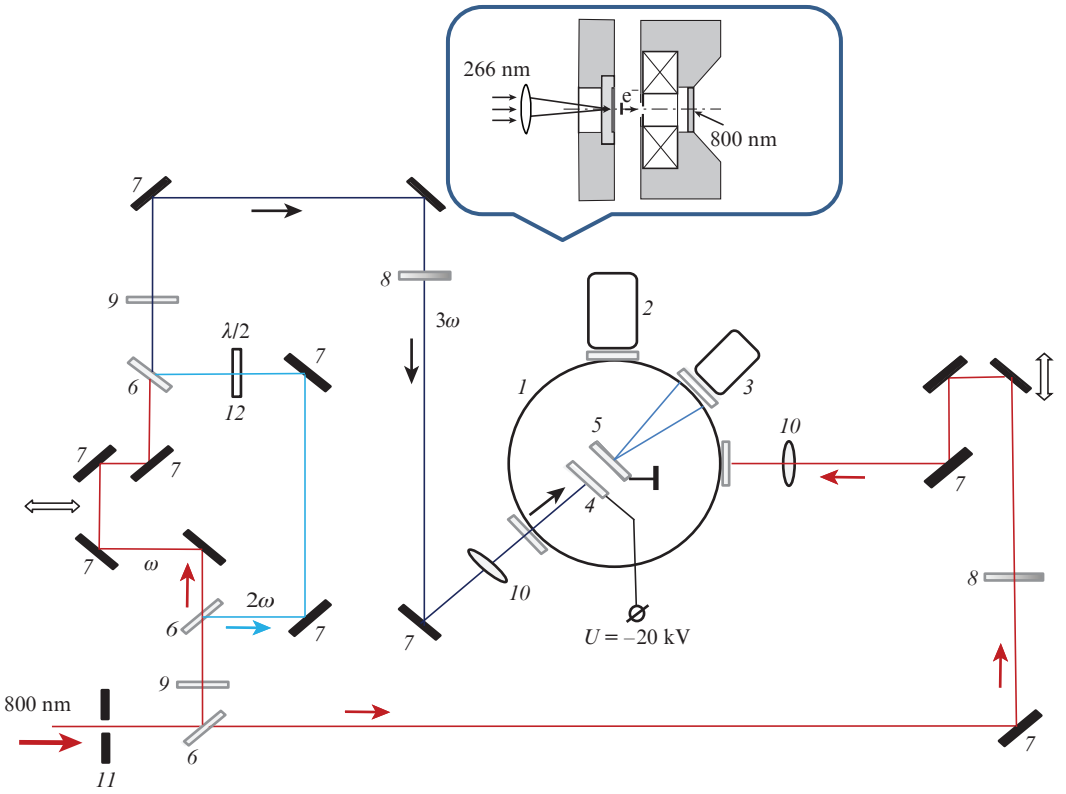

Figure 1. Schematic of a femtosecond electron diffractometer for experiments with thin films and nanoparticles: (*1*) vacuum chamber; (*2*) turbomolecular pump; (*3*) electron detector on the basis of microchannel plates, phosphor screen and CCD chamber; (*4*) gold photocathode; (*5*) anode + target; (*6*) beam splitters; (*7*) mirrors; (*8*) radiation attenuator; (*9*) converters of radiation into the second and third harmonics; (*10*) lenses; (*11*) diaphragm; (*12*) polarisation rotator. The inset shows the main elements of the device.

polycrystalline nature of the sample (Fig. 2a). Figure 2b shows the radial cross-section profile of the obtained electron diffraction pattern as a function of the scattering parameter $s = (4\pi/\lambda_{dB})\sin(\theta/2)$, where λ_{dB} is the electron wavelength, and θ is the scattering angle. Under our conditions, when the distance from the sample to the detector is approximately 208 mm, the radius of the detector is 20 mm, $\lambda_{dB} \approx 0.0859$ Å and the range of the recorded scattering parameter lies in the range $1.5\ Å^{-1} < s < 7\ Å^{-1}$. The lower limit is due to the size of the metal screen, which prevents the direct, undiffracted, photoelectron beam from reaching the detector. Diffraction maxima (1, –1, 0), (1, 1, –2) and (2, –2, 0) are observed against the background of smooth diffuse scattering mainly induced by thermal vibrations of Bi atoms, which are averaged under experimental conditions. Bismuth crystals in the film are oriented along the (111) axis of the rhombohedral system.

To produce a nonequilibrium state in the lattice, the sample was irradiated with high-power femtosecond laser radiation with a pulse energy density of about 2 mJ cm^{-2} and a repetition rate of 1 kHz. The characteristic depth of penetration of laser radiation at a wavelength of 0.8 μm into a bismuth sample is about 16 nm [16], which almost coincided with the thickness of our sample. The lateral size of the pump region (~1 mm) was larger than that of the probe region (~100 μm), which made it possible to minimise the effect of the laser pump nonuniformity. In the experiment, the electron diffraction pattern was recorded as a function of the delay time between the pump pulse and the probe pulse with a step

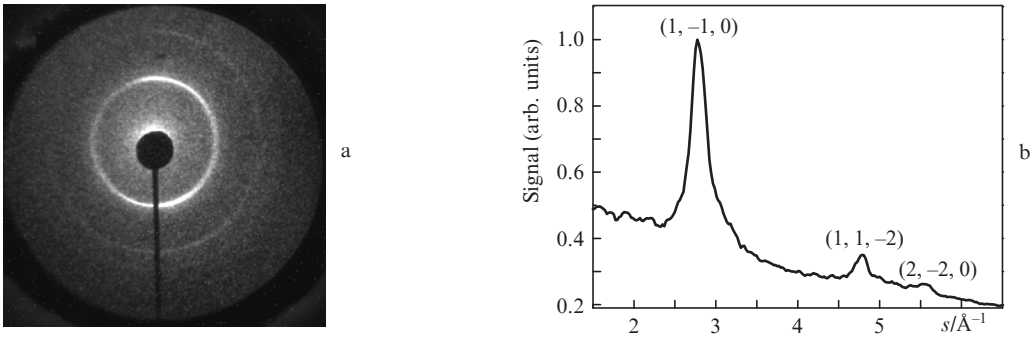

Figure 2. (a) Diffraction pattern of a thin bismuth film obtained using a pulsed photoelectron beam and (b) radial intensity profile for the cross section of the diffraction pattern. The designations of diffraction maxima are given in the rhombohedral system.

of 30 fs and an accumulation time of 2 s. The maximum time delay was about 10 ps. The obtained time dependence of the signal corresponding to the integrated intensity of the sector with a spanning angle of about 90° for the brightest ring in Fig. 2 was characterised by a set of oscillating components with characteristic periods on the subpicosecond scale (Fig. 3).

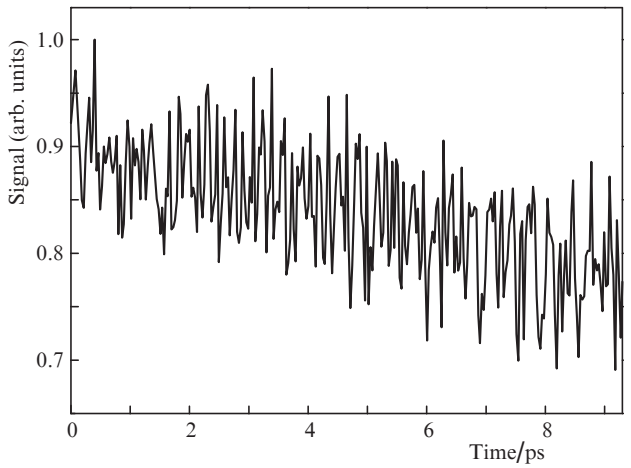

Figure 3. Dependence of the signal corresponding to the brightest ring of the electron diffraction pattern of Bi on the delay between the optical pump and probe photoelectron pulses.

3. Analysis of the results

It follows from the Fourier spectrum of the experimental data that the signal modulation is due to the presence of an ensemble of modes with pronounced frequencies of about 3, 6 and 9 THz (Fig. 4). Phonons at a frequency of 3 THz were previously recorded by the purely optical pump–probe technique [11–16]. This technique showed that this mode corresponds to fully symmetric A_{1g} optical lattice vibrations of bismuth atoms. The observed modes with higher frequencies are of particular interest, since they indicate nonlinear processes during the excitation of optical phonons in bismuth. Indeed, under our conditions, when intense femtosecond laser radiation is used to induce lattice oscillations, we can assume that

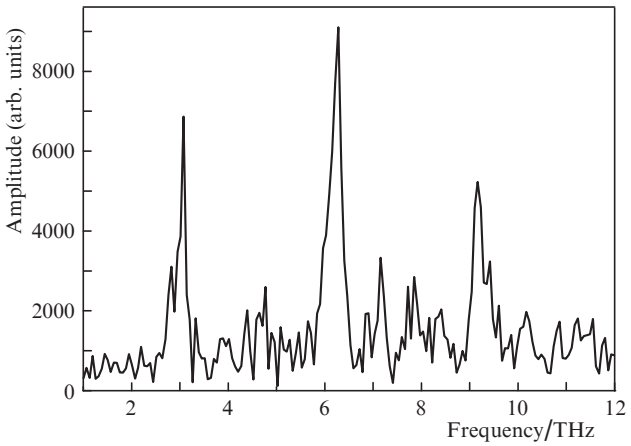

Figure 4. Fourier spectrum of laser-induced oscillations of the diffraction signal in a Bi-containing film.

lattice vibrations at frequencies of about 6 and 9 THz are manifestations of the first and second overtones of the three-terahertz peak. In this regard, we note that in studying bismuth with purely optical pump–probe methods, harmonics of optical phonons, including the second harmonic of the A_{1g} mode, have been previously detected under pumping the sample by high-energy laser pulses [11, 15]. As far as we know, the vibration frequency in the region of 9 THz for Bi crystallites has not been previously observed and can be related to the third harmonic of the A_{1g} phonon mode.

Compared to the first peak, Fig. 4 demonstrates a slightly higher intensity of the second peak corresponding to the position of the second harmonic of the A_{1g} mode. One of the possible reasons for this behaviour may be the presence of a thin oxide film on the surface of the sample. For example, optical phonons at a frequency of 6 THz were previously observed using Raman spectroscopy for α and β polymorphs of bismuth oxide Bi_2O_3 [22].

Detection of rapidly oscillating coherent optical phonons using UED requires a rather high temporal resolution, which depends mainly on the probe channel [1–6]. The duration of photoelectron pulses is determined by two main mechanisms. First, acceleration of photoelectrons in a static electric field near the cathode causes the electron bunch to elongate by the value of the time-of-flight chromatic aberration τ_F [4, 23], which is associated with the initial spread of the kinetic energy of electrons, but does not depend on the Coulomb interaction of charges in the beam:

$$\tau_F = \frac{\sqrt{2m_e\delta E}}{eF}, \tag{1}$$

where m_e and e are the mass and charge of the electron; δE is the distribution width of the initial kinetic energy of the photoelectrons; and F is the electric field strength in the accelerating gap. Under our conditions, at $\delta E \approx 0.4$ eV and $F = 6.7\times10^6$ V m^{-1}, the time-of-flight chromatic aberration is $\sim$320 fs.

The second mechanism leading to electron pulse broadening is due to the Coulomb repulsion of charges, which depends on the propagation time of the electron beam. For the calculation, we use formulae (19) and (22) from [24], which describe the Coulomb broadening of the electron pulse in the accelerating gap of the device (τ_{C1}) and when the electron pulse accelerated to 20 keV drifts from the anode to the sample (τ_{C2}):

$$\tau_{C1} = \frac{4l^2N\sqrt{em_e}}{\pi\sqrt{2U^3}\varepsilon_0 d^2}, \tag{2}$$

$$\tau_{C2} = \frac{L^2N\sqrt{em_e}}{\pi\sqrt{2U^3}\varepsilon_0 d^2}, \tag{3}$$

where l is the length of the accelerating gap; L is the length of the path travelled by the beam from the anode to the sample; N is the number of electrons per pulse; U is the voltage on the accelerating gap; d is the beam diameter; and ε_0 is the electric constant. For estimates, we take the following parameters of a compact device: $l = 3$ mm, $L = 9$ mm, $U \approx 2\times10^4$ V, $N \approx 1000\pm300$ (the number of electrons in the bunch fluctuates over time as a function of energy in the laser pulse irradiating the photocathode), and $d = 100$ μm. As a result, we have $\tau_{C1} \approx 12\pm4$ fs and $\tau_{C2} \approx 28\pm9$ fs. Summing up the contributions described by formulae (1)–(3), we obtain $\tau_p \approx 360 \pm 12$ fs,

which implies that the duration of the probe pulses during the experiment remains almost unchanged.

Thus, coherent oscillations of the lattice in a thin film were initiated by femtosecond laser radiation, which made it possible to obtain coherent phonons with frequencies up to about 10 THz determined by the width of the spectrum of a laser pulse with a duration of 50 fs. The use of short electronic pulses, stable in duration and strictly synchronised in time, ensured a high degree of details in the experiment at a sufficiently small (at a level of several tens of femtoseconds) scanning step, which is confirmed by the obtained data.

4. Conclusions

The detection of consistent vibrations of atoms with a high degree of spatiotemporal coherence is a powerful tool for studying matter under nonstationary conditions. The UED method is capable of visualising the behaviour of condensed matter in real time at various stages of vibrational motion, which significantly expands the feasibility of studying the crystalline lattice, allowing one to analyse energy transfer, interaction of vibrational modes and other processes, the study of which in traditional spectroscopy is a challenging task.

It is known that classical electron diffraction makes is possible to visualise the positions of nuclei in a crystalline lattice with high accuracy reaching $\sim 10^{-2}$ Å. Using a femtosecond laser for pulsed excitation of matter and generation of laser-induced atomic–molecular motion in the sample itself, as well as for the formation of ultrashort probe electron bunches provides a temporal resolution of ~100 fs. Such a combination of spatiotemporal characteristics is the basis for observing 'atomic–molecular cinema' in matter, and this study is an important step in this direction.

In our experiment using a compact ultrafast electron diffractometer, we detected optical phonons with record high (for UED) frequencies (up to ~9 THz), which can serve as a demonstration of nonlinear phononics in a thin Bi film under the action of high-power femtosecond laser radiation. Note that, as far as we know, the third harmonic of the A_{1g} mode in bismuth has not been previously observed. The lack of literature data on the generation of the third harmonic of the A_{1g} mode in this material suggests that our results are probably due to quantum confinement in a 20-nm Bi nanostructure.

Shin et al. [16] performed a comparative study of bulk and thin-film (with thicknesses in the range of 25–40 nm) bismuth samples by femtosecond laser spectroscopy in reflection mode. When working with films, the proximity of the characteristic transverse size of the nanostructure to the depth of light penetration made it difficult to observe quantum confinement in this material due to the reflection of the probe laser beam from the back surface of the film [16].

The use of a transmission electron probe allows one to overcome this limitation. Note that the characteristic mean free path of electrons in a solid increases with increasing kinetic energy of the electron beam and, for example, reaches ~100 nm in the relativistic case. This opens up the possibility of a detailed study of the quantum size effect [20, 21] in thin Bi films in a wide range of thicknesses by the UED method.

Acknowledgements. The experiments were performed at the Unique Scientific Facility 'Multipurpose Femtosecond Laser Diagnostic Spectrometric Complex' of the Institute for Spectroscopy of the Russian Academy of Sciences. This work was supported by the Russian Foundation for Basic Research (Grant No. 20-02-00146 A).

References

1. Zewail A.H., Thomas J.M. *4D Electron Microscopy. Imaging in Space and Time* (London: Imperial College Press, 2010).
2. Ishenko A.A., Girichev G.V., Tarasov Yu.I. *Diffraktsiya elektronov: Struktura i dinamika svobodnykh molekul i kondensirovannogo sostoyaniya veshchestva* (Electron Diffraction: Structure and Dynamics of Free Molecules and The Condensed State of Matter) (Moscow: Fizmatlit, 2013).
3. Ischenko A.A., Aseyev S.A. *Time Resolved Electron Diffraction: for Chemistry, Biology and Materials Science* (USA, San Diego: Elsevier, 2014).
4. Ischenko A.A., Aseyev S.A., et al. *Usp. Fiz. Nauk*, **184**, 681 (2014).
5. Ischenko A.A., Weber P.M., Miller R.J.D. *Chem. Rev.*, **117**, 11066 (2017).
6. Aseyev S.A., Ryabov E.A. *Usp. Fiz. Nauk*, **189**, 306 (2019).
7. Mironov B.N., Kompanets V.O., et al. *JETP Lett.*, **103**, 531 (2016) [*Pis'ma Zh. Eksp. Teor. Fiz.*, **103**, 597 (2016)].
8. Mironov B.N., Kompanets V.O., et al. *JETP*, **124** (3), 422 (2017) [*Zh. Eksp. Teor. Fiz.*, **151** (3), 494 (2017)].
9. Hofmann Ph. *Progress in Surface Science*, **81**, 191 (2006).
10. Ishioka K., Misochko O.V., in *Progress in Ultrafast Intense Laser Science V*. Ed. by K. Yamanouchi, A. Giullietti, K. Ledingham (Berlin, 2010) Springer Series in Chem. Phys., pp 23–64.
11. Misochko O.V., Hase M., Kitajima M. *JETP Lett.*, **78**, 75 (2003) [*Pis'ma Zh. Eksp. Teor. Fiz.*, **78**, 85 (2003)].
12. Mel'nikov A.A., Misochko O.V., Chekalin S.V. *JETP Lett.*, **89**, 129 (2009) [*Pis'ma Zh. Eksp. Teor. Fiz.*, **89**, 147 (2009)].
13. Misochko O.V., Ishioka K., et al. *Phys.: Condens. Matter*, **18**, 10571 (2006).
14. Chekalin S.V., Melnikov A.A., Misochko O.V. *Laser Phys.*, **24**, 094004 (2014).
15. Misochko O.V. *JETP*, **118**, 227 (2014) [*Zh. Eksp. Teor. Fiz.*, **145**, 262 (2014)].
16. Shin T., Wolfson J.W., et al. *Phys. Rev. B*, **92**, 184302 (2015).
17. Shin T. *Current Appl. Phys.*, **19**, 256 (2019).
18. Sciaini G., Harb M., Kruglik S.G., et al. *Nature*, **458**, 56 (2009).
19. Bugayev A., Elsayed-Ali H.E. *J. Phys. Chem. Solids*, **129**, 312 (2019).
20. Rogacheva E.I., Grigorov S.N., et al. *Appl. Phys. Lett.*, **82**, 2628 (2003).
21. Rogacheva E.I., Lyubchenko S.G., Dresselhaus M.S. *Thin Solid Films*, **516**, 3411 (2008).
22. Steele J.A., Lewis R.A. *Opt. Mater. Express*, **4** (10), 2133 (2014).
23. Aseyev S.A., Sadkov A.S., et al. *JETP*, **128**, 379 (2019) [*Zh. Eksp. Teor. Fiz.*, **155** (3), 440 (2019)].
24. Qian B-L., Elsayed-Ali H.E. *J. Appl. Phys.*, **91**, 462 (2002).